Surface-gated quantum Hall effect in an InAs heterostructure

Ian J. Gelfand[a)]
Division of Engineering and Applied Sciences, Harvard University, Cambridge, Massachusetts 02138

S. Amasha, D. M. Zumbühl, and M. A. Kastner
Department of Physics, Massachusetts Institute of Technology, Cambridge, Massachusetts 02139

C. Kadow and A. C. Gossard
Department of Materials Science and Engineering, University of California, Santa Barbara, Santa Barbara, California 93106

(Received 16 December 2005; accepted 24 April 2006; published online 19 June 2006)

We demonstrate low leakage surface gating of an indium arsenide heterostructure with the two-dimensional electron gas close to the surface. Gating is made possible by growing an aluminum oxide layer on top of the device. We find that the depletion point can be changed by applying a positive gate voltage and we see hysteresis when the voltage is swept below depletion. © *2006 American Institute of Physics*. [DOI: 10.1063/1.2210289]

InAs–AlSb quantum wells have been studied for several years.[1–7] Engineers are interested in them because the system's high electron density allows for fast switching times, making them useful for high frequency circuits.[8–10] Physicists are interested in them because of the high g factor, low effective mass, and strong spin-orbit coupling of electrons in InAs.[11–13] Additionally, the high g factor would result in strong coupling to microwave magnetic fields, which might be useful for applications to quantum computing.[14]

A major impediment in the creation of devices with this system is the difficulty in gating it. Whereas putting a metal gate directly on GaAs produces a Schottky barrier, doing this to InAs produces low resistance contacts.[1,15] Although the gate leakage can be acceptable in some engineering applications,[9] it prohibits the formation of quantum dots and other interesting structures. We have circumvented this by growing a high-quality, atomic layer deposition (ALD) aluminum oxide film over our structure,[16] which allows us to vary the electron density in an InAs quantum well over a large range. Although surface gating of InAs heterostructures has been reported, attempts to form Schottky barriers have resulted in large gate leakage currents.[2] Back gating of InAs has been reported previously[6] and surface gating with a dielectric layer has been successful.[17] However, in the latter work the two-dimensional electron gas (2DEG) is nearly 500 nm below the surface. The length scales for single electron dots typically require the 2DEG depth to be no more than ~150 nm, so this method is incompatible with making single electron nanostructures. The 2DEG in our sample is 74 nm below the surface, significantly less than that needed to make quantum dots.[18]

Our starting material has the following structure starting from the bottom. A semiinsulating GaAs substrate, 1 μm of GaAs followed by 10 nm AlAs and 10 μm of AlSb as nucleation layers, and a 1.5 μm $Ga_{0.2}Al_{0.8}Sb$ isolation floor which separates the nucleation layer from the electrically active part of the heterostructure. The latter consists of (Fig. 1, inset) a 30 nm AlSb bottom barrier, a 13 nm InAs quantum well, a 20 nm AlSb top barrier, and a 7.5 nm GaSb cap layer. The cap layer prevents the AlSb from oxidizing. The AlSb top barrier contains a 10^{12} cm^{-2} delta doping layer of beryllium to act as an electron acceptor.[19]

Because of the sensitivity of the GaSb cap layer to chemicals normally used in photolithography, we have used electron beam lithography to define Hall bars. After patterning polymethyl methacrylate (PMMA), we etch our GaSb cap layer and AlSb barrier with ammonium hydroxide and we etch the InAs quantum well with acetic acid/hydrogen peroxide down through to the bottom AlSb barrier. The InAs quantum well is then undercut with a citric acid/peroxide etchant.

Ohmic contacts are formed with a Pd/Ti/Pd/Au metallization and lift-off process and annealed at 180 °C for 15 min. Electron beam lithography is then used to open holes in PMMA over the mesa prior to ALD growth of oxide. The mesa is covered with a 30 nm thick Al_2O_3 oxide layer, which

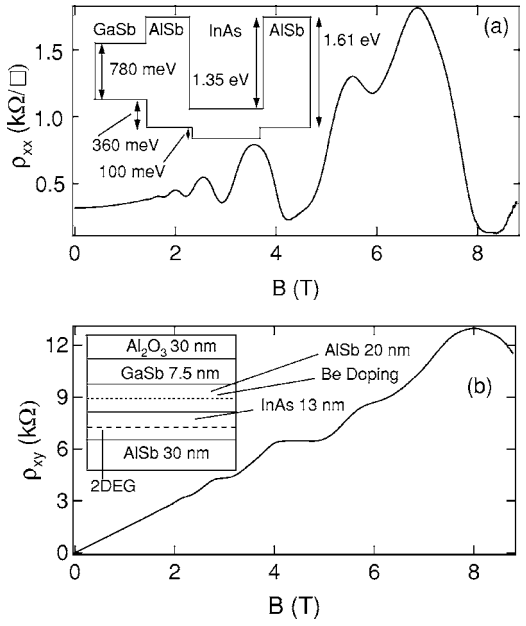

FIG. 1. (a) Longitudinal magnetoresistance in the InAs–AlSb double barrier heterostructure with $V_g=0$. (Inset) energy bands vs depth for the InAs–AlSb double barrier heterostructure (adapted from Ref. 1). (b) Hall resistance measured simultaneously. (Inset) layer structure of material used in this study.

[a)]Electronic mail: igelfand@fas.harvard.edu

covers the side walls as well as the top surface of the mesa. The ALD film is grown by introducing water into a steel chamber heated to 120 °C; the high temperature ensures that only a monolayer of water stays on the sample. Trimethylaluminum is introduced into the chamber and reacts with the water to form a nominally monolayer-thick film of alumina. The film is built up one monolayer at a time until we have the desired thickness. Gates are formed from Pd/Ti/Au using a standard electron beam lithography lift-off process. In our low leakage gated Hall bars, we see leakage currents of ~100 pA at ±15 V and <50 pA at ±5 V. Roughly 60% of the gated Hall bars, which are 60×400 μm^2, show this low leakage.

The gated Hall bars are cooled to 430 mK in a helium-3 refrigerator and measured in magnetic fields up to 8.8 T. Figure 1 shows measurements on a typical Hall bar with zero voltage on the gate. All measurements performed here are made in a four-probe configuration with an applied dc current of 1 μA. We see clear oscillations in the longitudinal magnetoresistance and plateaus in the Hall resistance. Analysis of the Shubnikov–de Haas oscillations at fields below ~4 T gives an electron sheet density of $4.3\pm0.1\times10^{11}$ cm^{-2}. The low field Hall data give a value of $4.29\pm0.01\times10^{11}$ cm^{-2}. Using this we find the device mobility to be $45\,000\pm1000$ cm^2/V s. This compares to $n=5\times10^{11}$ cm^{-2} and $\mu=35\,000$ cm^2/V s found in previous measurements on the same material.[19]

Above 8 T the Hall resistance begins to decrease. This is similar to the behavior observed by Hopkins *et al.* in a nongated InAs–AlSb heterostructure.[20] We speculate that this may be the result of disorder in the system, which becomes more important for low filling factors.

Upon first variation of gate voltage we find large hysteresis in Hall and longitudinal resistances. However, after sweeping repeatedly between $V_g=0$ and +4 V, the hysteresis becomes small, except in the region below threshold as discussed below. This cycling of the sample in the range $0\text{ V}<V_g<+4$ V also shifts the threshold from about −1 to about +1 V. This is consistent with earlier observations.[2]

After voltage cycling, measurements in a high magnetic field show a gate-induced quantum Hall effect, like that seen in Si metal-oxide-semiconductor field-effect transistors (MOSFETs).[21] Figure 2 shows well defined plateaus in Hall resistance and very small longitudinal resistance at the plateaus at the highest fields. The data in Fig. 2 are from a different sample than in Fig. 1. Shown here are traces from $V_g=+4$ V to $V_g=+1.8$ V (down sweep); traces in the upsweep direction do not lie exactly on top of these. One clearly sees that the plateaus become better resolved with increasing field, and the spin splitting is resolved above 6 T.

From the ρ_{xx} and ρ_{xy} data at $B=2$ T in Fig. 2, it is possible to extract estimates of density and mobility as a function of gate voltage [Fig. 2(c)]. Ideally, mobility and density would be calculated in the small Hall angle limit. However, at 2 T we see no evidence of Hall plateaus and only very weak Shubnikov–de Haas oscillations, allowing us to estimate the mobility. Density is calculated from $n_{2D}=B/e\rho_{xy}$ and mobility from $\mu=1/(n_{2D}e\rho_{xx})$; we use the size of the oscillations in ρ_{xx} at 2 T to calculate the error bars. Mobility is seen to increase from ~50 000 cm^2/V s at $V_g=+1.6$ V to ~150 000 cm^2/V s at $V_g=+3.8$ V.

As discussed above, sweeping the gate below the depletion point causes hysteresis. Figure 3 shows sweeps over

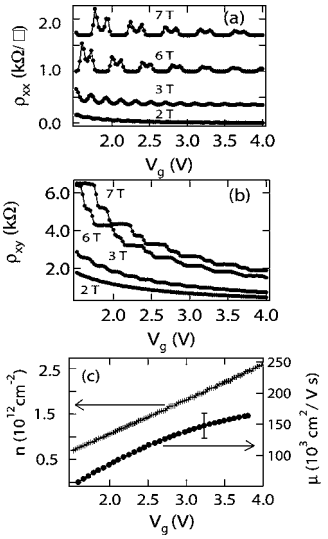

FIG. 2. (a) Longitudinal and (b) Hall resistance as functions of gate voltage. Data, from bottom to top, are for $B=2$, 3, 6, and 7 T. The longitudinal resistance data are offset by 0, 350, 100, and 1700 Ω from bottom to top. The lines between points are guides to the eye. The single periodicity in ρ_{xx} as a function of gate voltage implies a single occupied subband for the voltage range tested. Electron concentration in the well before application of gate voltages is $n=4.2\pm0.1\times10^{11}$ cm^{-2}. (c) shows density and mobility as a function of gate voltage. Error bars for mobility are ±20,000 cm^2/V s.

plateaus in Hall resistance corresponding to $\rho_{xy}\sim h/e^2$ (near 1.1 V) and $\rho_{xy}\sim h/2e^2$ (between 1.2 and 1.4 V). Hysteresis is most pronounced in the Hall data below $\nu=1$. That ρ_{xy} is slightly below h/e^2 while ρ_{xx} is nonzero for $\nu=1$ suggests that the spin splitting is incomplete at 7 T. The hysteresis is small except when the voltage is varied below $\nu=1$.

In Fig. 3 one sees that both ρ_{xx} and ρ_{xy} increase and become hysteretic as V_g is decreased below the threshold near 1 V. To explore the time scale of the hysteresis we have measured the response to a gate voltage step. The inset in Fig. 3 shows ρ_{xx}, beginning with V_g set ~200 mV above threshold; after ~220 s, V_g is decreased to 400 mV below threshold. When V_g is stepped, ρ_{xx} increases by a factor of ~30, but is then stable in time for 200 s. We observe

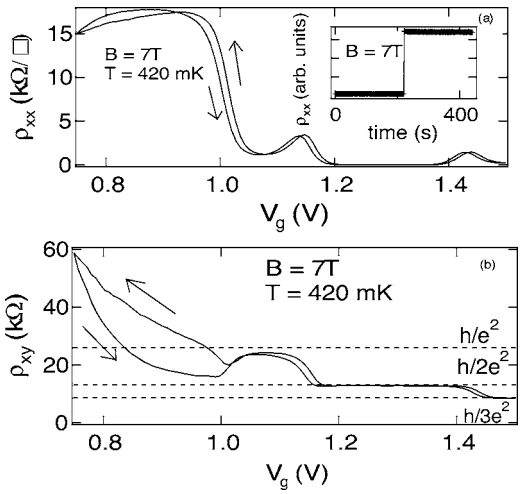

FIG. 3. Longitudinal and Hall resistance as functions of gate voltage near depletion. Below depletion hysteresis becomes large. Above depletion the up and down traces are very reproducible. (Inset) when the gate voltage is stepped from ~200 mV above depletion to ~400 mV below depletion, ρ_{xx} increases by a factor of 30 and is stable in time for 200 s.

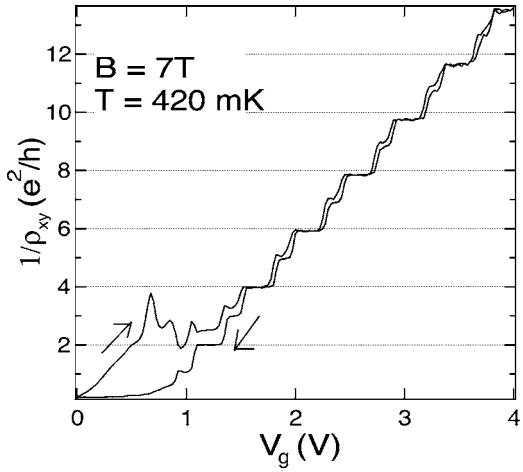

FIG. 4. Reciprocal of Hall resistance vs gate voltage at $B=7$ T and $T=420$ mK. We see well defined steps from $\nu=1$ to $\nu>12$. The up and down traces are very reproducible if V_g is kept above depletion; below depletion the data are hysteretic. We deplete down to $\rho_{xy}^{-1}\sim 0.2e^2/h\sim 129$ kΩ.

changes in ρ_{xx} on this time scale only when V_g is stepped by ~1 V below threshold. Although more work must be done to understand the nature of the hysteresis, the stability of ρ_{xx} when the quantum well is depleted for hundreds of seconds is a hopeful sign for this material's eventual role in making surface-gated nanostructures.

Figure 4 shows well defined steps in ρ_{xy}^{-1} from $\rho_{xy}^{-1}\sim 14e^2/h$ down to $\rho_{xy}^{-1}=e^2/h$. Although the data in Fig. 4 come from the same sample studied in Fig. 3, they are taken in a separate measurement. Surprisingly, the ρ_{xy}^{-1} plateaus begin to fall below the integer multiples of e^2/h for $\rho_{xy}^{-1}>7e^2/h$. This deviation is not observed at $B=6$ T, and the origin of the deviation at 7 T is unclear. The highest density we have obtained is roughly 2.3×10^{12} cm^{-2}. Nguyen *et al.*[17] have observed a change in the period of magnetocapacitance oscillations and a decrease in the low field mobility with increasing density at approximately half this concentration; they have interpreted these observations as manifestations of occupancy of a second subband. Surprisingly, we see no evidence of a change in period in our magnetoresistance oscillations (Fig. 2) and no decrease in the mobility over the large range of densities we have studied. We do not understand why the second subband occupancy does not affect these measurements. We speculate that occupancy of the second subband may be related to the Hall conductance falling below ne^2/h at 7 T, but understanding this relationship requires further study.

As seen in Figs. 3 and 4, we are able to reduce the density at low voltage, leading to $1/\rho_{xy}$ as low as $0.2e^2/h$ or 7.76 μS (resistance of 129 kΩ), but we are unable to make the resistance larger than this by further reduction of V_g. Koester *et al.*[2] have reported a residual conductance of 20–70 μS in InAs–AlSb quantum point contact devices.

We have demonstrated surface gating of InAs–AlSb heterostructures with low gate leakage. We anticipate that this is a first step to making surface-gated InAs nanostructures.

The authors are grateful to C. Marcus and E. Laird for assistance in ALD growth and T. Greytak and G. Steele for helpful advice. This work has been supported primarily by the NSEC program of the National Science Foundation under Award No. PHY-0117795 and in part by NSF Award No. DMR-0353209 and ARO Grant No. W911NF-05-1-0062. Two of the authors (C.K.) and (A.G.) acknowledge support from DARPA's ABCS program Contract No. N66001-01-C-8032.

[1] H. Kroemer, Physica E (Amsterdam) **20**, 196 (2004).
[2] S. J. Koester, B. Brar, C. R. Bolognesi, E. J. Caine, A. Patlach, E. L. Hu, and H. Kroemer, Phys. Rev. B **53**, 13063 (1996).
[3] S. J. Koester, C. R. Bolognesi, M. J. Rooks, E. L. Hu, and H. Kroemer, Appl. Phys. Lett. **62**, 1373 (1993).
[4] S. Brosig, K. Ensslin, A. G. Jansen, C. Nguyen, B. Brar, M. Thomas, and H. Kroemer, Phys. Rev. B **61**, 13045 (2000).
[5] T. P. Smith III and F. F. Fang, Phys. Rev. B **35**, 7729 (1987).
[6] F. C. Wang, W. E. Zhang, C. H. Yang, M. J. Yang, and B. R. Bennett, Appl. Phys. Lett. **69**, 1417 (1996).
[7] Yu. Sadofyev, A. Ramamoorthy, B. Naser, J. P. Bird, S. R. Johnson, and Y. H. Zhang, Appl. Phys. Lett. **81**, 1833 (2002).
[8] J. B. Boos, Walter Kruppa, Brian R. Bennett, Doewon Park, Steven W. Kirchoefer, Robert Bass, and Harry B. Dietrich, IEEE Trans. Electron Devices **45**, 1869 (1998).
[9] C. Kadow, M. Dahlstroem, J.-U. Bae, H.-K. Lin, A. C. Gossard, M. J. W. Rodwell, B. Brar, G. J. Sullivan, G. Nagy, and J. I. Bergman, IEEE Trans. Electron Devices **52**, 151 (2005).
[10] M. J. Yang, K. A. Cheng, C. H. Yang, and J. C. Culbertson, Appl. Phys. Lett. **80**, 1201 (2002).
[11] C. Hermann and C. Weisbuch, Phys. Rev. B **15**, 823 (1977).
[12] J. Nitta, T. Akazaki, H. Takayanagi, and T. Enoki, Phys. Rev. Lett. **78**, 1335 (1997).
[13] T. Koga, J. Nitta, T. Akazaki, and H. Takayanagi, Phys. Rev. Lett. **89**, 046801 (2002).
[14] H. A. Engel and D. Loss, Phys. Rev. B **65**, 195321 (2002).
[15] B. Streetman, *Solid State Electronic Devices* (Prentice-Hall, Upper Saddle River, NJ, 1995).
[16] M. J. Biercuk, D. J. Monsma, and C. M. Marcus, Appl. Phys. Lett. **83**, 2405 (2003).
[17] C. Nguyen, K. Ensslin, and H. Kroemer, Surf. Sci. **267**, 549 (1992).
[18] G. Granger, M. A. Kastner, I. Radu, M. P. Hanson, and A. C. Gossard, Phys. Rev. B **72**, 165309 (2005).
[19] C. Kadow, H.-K. Lin, M. Dahlstroem, M. Rodewll, A. C. Gossard, B. Brar, and G. Sullivan, J. Cryst. Growth **251**, 543 (2003).
[20] P. F. Hopkins, A. J. Rimberg, R. M. Westervelt, G. Tuttle, and H. Kroemer, Appl. Phys. Lett. **58**, 1428 (1991).
[21] F. F. Fang and P. J. Stiles, Phys. Rev. B **27**, 6487 (1983).